Advances in Applied Mathematics and Mechanics
Adv. Appl. Math. Mech., Vol. **6**, No. 2, pp. 220-232

DOI: 10.4208/aamm.2013.m93
April 2014

Axisymmetric Stagnation-Point Flow of Nanofluid Over a Stretching Surface

M. Nawaz[1,*] and T. Hayat[2,3]

[1] *Department of Humanities and Sciences Institute of Space Technology, P.O. Box 2750, Islamabad 44000, Pakistan*
[2] *Department of Mathematics, Quaid-i-Azam University 45320 Islamabad 44000, Pakistan*
[3] *Department of Mathematics, Faculty of Sciences, King Abdulaziz University, Jeddah 80253, Saudi Arabia*

Received 17 January 2013; Accepted (in revised version) 18 July 2013

Available online 3 April 2014

Abstract. This paper investigates the laminar boundary layer flow of nanofluid induced by a radially stretching sheet. Nanofluid model exhibiting Brownian motion and thermophoresis is used. Series solutions for a reduced system of nonlinear ordinary differential equations are obtained by homotopy analysis method (HAM). Comparative study between the HAM solutions and previously published numerical results shows an excellent agreement. Velocity, temperature and mass fraction are displayed for various values of parameters. The local skin friction coefficient, the local Nusselt number and the local Sherwood number are computed. It is observed that the presence of nanoparticles enhances the thermal conductivity of base fluid. It is found that the convective heat transfer coefficient (Nusselt number) is decreased with an increase in concentration of nanoparticles whereas Sherwood number increases when concentration of nanoparticles in the base fluid is increased.

AMS subject classifications: 76D10, 80A20

Key words: Nanofluid, axisymmetric flow, stagnation point, Nusselt number, Sherwood number.

1 Introduction

There has been an increasing interest of the recent researchers in the flows induced by a stretching surface. This is because of extensive applications of such flows in polymer processing, metallurgy, drawing of plastic sheets, cable coating, continuous casting, glass blowing, spinning synthetic fibers etc. Since the pioneering work of Crane [1] on the

*Corresponding author.
Email: nawaz_d2006@yahoo.com (M. Nawaz)

titled problem, the two-dimensional flows caused by a stretching sheet have been examined under various aspects (see [1–5]) and several References therein). However it is noted that flows generated by radially stretching surface is scarce. For instance, Ariel [2] analyzed slip effects on axisymmetric flow of viscous fluid induced by a stretching surface. Hayat et al. [3] considered axisymmetric unsteady flow of micropolar fluid between radially stretching surfaces. Hayat et al. [4] discussed thermal-diffusion and diffusion-thermo effects on axisymmetric flow of second grade fluid between radially stretching surfaces. Hayat and Nawaz [5] investigated axisymmetric flow between radially stretching surfaces. The studies [2–5] and several References therein are restricted to axisymmetric flows of Newtonian and non-Newtonian fluids and no study regarding axisymmetric flow of nanofluids over a radially surface is investigated so far. Therefore present investigation is an attempt in this direction. Literature survey also reveals that no study regarding stagnation point flow of nanfluid over a radially stretching sheet is discussed so far. However several studies on stagnation point flow of other than nanofluids are conducted. For example, stagnation point flows towards a stretching sheet are also studied by the researchers. The stagnation point flow of viscous fluid over a stretching surface has been addressed by Chiam [6]. Mahapatra et al. [7] considered stagnation point flow of power-law fluid towards a stretching surface. Labropulu and Li [8] studied slip effects on stagnation point flow of second grade fluid. Numerical solution for stagnation point flow of viscous fluid over a radially stretching surface has been computed by Attia [9]. Mixed convection in the stagnation point flow towards a stretching vertical permeable sheet is considered by Ishak et al. [10]. The unsteady stagnation-point flow driven by rotating disk has been examined by Hayat and Nawaz [11].

Recently, the flow analysis of nanofluids has been the topic of great interest due to their occurrence in nuclear reactors, transportation, biomedicine etc. Actually many ordinary fluids including water, toluene, ethylene glycol and mineral oils etc. are commonly used in cooling processes in industry. These fluids have poor thermal characteristics. Experimental and theoretical investigations show that the inclusion of micro-scaled particles in the base fluids enhances their thermal conductivity. Such mixture of the fluids and nanoparticles are called nanofluids. Perhaps, Choi [12] was the first to use the word nanofluid. It is known fact now that presence of nanoparticles in base fluid improves its thermal conductivity. Furthermore, nanofluids show better stability and rheological properties in comparison with base fluid. At present, the reasonable literature on nanofluids is available. For example, Masuda et al. [13] studied the effects of ultra fine particles on thermal conductivity of the base fluid. Das [14] concluded that thermal conductivity of the base fluid can be enhanced by injecting nanoparticles into it. The transfer of heat in fluid containing metallic oxide particles (nanoparticles) has been studied by Pak and Cho [15]. Eastman et al. [16] noted an increase in thermal conductivity of ethylene-glycol containing nanoparticles. Effects of nanoparticles on thermal conductivity of water have been investigated by Minsta [17]. Razi et al. [18] studied the pressure drop and heat transfer of nanofluid flow inside horizontal flattened tubes. Mixed convection of a nanofluid in an inclined enclosure cavity is discussed by Alinia et al. [19]. Rana and Bhargava [20] examined heat transfer in two-dimensional flow of nanofluid over a nonlinear stretching surface. Hamad and Ferdows [21] developed similarity solution for flow of nanofluid induced by a porous stretching sheet.

Shortly, the purpose of present study is two fold. (i) to investigate the axisymmetric flow of nanofluid over a stretching surface (ii) to take into account the radial type free stream velocity $U_e(r)=ar$. The present communication is managed as follows. First the relevant mathematical problem is formulated. Governing nonlinear problems are solved for the series solutions by using recent developed technique namely homotopy analysis method (HAM). This is a novel technique and has been already employed to solve many nonlinear problems. Some of these studies can be mentioned through the References (Liao [22], Rashidi et al. [23], Abbasbandy and Shirzadi [24], Hayat et al. [25], Hashim et al. [26]). Convergence of series solutions is ensured. The mathematical solutions are analyzed by plots and tables.

2 Mathematical formulation

We consider stagnation-point axisymmetric flow of nanofluid over a radially stretching surface. Nanofluid occupies the half space $z\geq 0$. The sheet is maintained at constant temperature T_w and C_w (the nanoparticle mass fraction) at the surface of stretching sheet. T_∞ and C_∞ denote the ambient temperature and nanoparticle mass fraction respectively. The velocity components in the flow near the stagnation point are given by $U_e(r)=ar$, $W_e(z)=-2az$ and velocity of stretching sheet is $U_w(r)=cr$ where a and c are the positive constants. The relevant boundary layer flow equations are

$$\frac{\partial u}{\partial r}+\frac{u}{r}+\frac{\partial w}{\partial z}=0, \tag{2.1a}$$

$$u\frac{\partial u}{\partial r}+w\frac{\partial u}{\partial z}=U_e\frac{dU_e}{dr}+\nu\Big(\frac{\partial^2 u}{\partial z^2}\Big), \tag{2.1b}$$

$$u\frac{\partial T}{\partial r}+w\frac{\partial T}{\partial z}=\alpha\Big(\frac{\partial^2 T}{\partial z^2}\Big)+\tau\Big\{D_B\Big(\frac{\partial C}{\partial z}\frac{\partial T}{\partial z}\Big)+\frac{D_T}{T_\infty}\Big(\frac{\partial T}{\partial z}\Big)^2\Big\}, \tag{2.1c}$$

$$u\frac{\partial C}{\partial r}+w\frac{\partial C}{\partial z}=D_B\Big(\frac{\partial^2 C}{\partial z^2}\Big)+\frac{D_T}{T_\infty}\frac{\partial^2 T}{\partial z^2}, \tag{2.1d}$$

with the following boundary conditions

$$\left.\begin{array}{l} u=U_w(r)=cr, \quad w=0, \quad T=T_w, \quad C=C_w \quad \text{at } z=0, \\ u\to U_e(r)=ar, \quad T\to T_\infty, \quad C\to C_\infty \quad \text{as } z\to\infty, \end{array}\right\} \tag{2.2}$$

where u and w are the velocity components along the radial (r) and axial (z) directions respectively, T is the temperature of the fluid, C is the mass fraction field, ν $(=\mu/\rho_f)$ is the kinematic viscosity, ρ_f is the density of the fluid, μ is the dynamic viscosity, α is the thermal diffisivity, D_B is the Brownian diffusion coefficient, D_T is the thermophoretic coefficient, $\tau=(\rho c)_p/(\rho c)_f$, $(\rho c)_p$ and $(\rho c)_f$ are the volumetric expansion coefficients and ρ_p is the density of the nanoparticles.

Invoking the following relations

$$u=crf'(\eta),\quad w=-2\sqrt{c\nu}f(\eta),\quad \theta(\eta)=\frac{T-T_\infty}{T_w-T_\infty},\quad \phi(\eta)=\frac{C-C_\infty}{C_w-C_\infty},\quad \eta=\sqrt{\frac{c}{\nu}}z, \tag{2.3}$$

Eqs. (2.1a)-(2.2) are reduced to

$$\left.\begin{aligned}&f'''+2ff''-f'^2+A^2=0,\\&f'(\eta)=1,\quad f(\eta)=0,\quad f'(\infty)=A,\end{aligned}\right\} \tag{2.4a}$$

$$\left.\begin{aligned}&\theta''+\mathrm{Pr}(2f\theta'+N_b\theta'\phi'+N_t(\theta')^2)=0,\\&\theta(0)=1,\quad \theta(\infty)=0,\end{aligned}\right\} \tag{2.4b}$$

$$\left.\begin{aligned}&\phi''+2Lef\phi'+\frac{N_t}{N_b}\theta''=0,\\&\phi(0)=1,\quad \phi(\infty)=0,\end{aligned}\right\} \tag{2.4c}$$

where $A=a/c$ is the ratio of free stream velocity to the velocity of stretching sheet, Le is the Lewis number, N_b is the Brownian motion parameter, Pr is the Prandtl number and N_t is the thermophoresis parameter. These are defined

$$Le=\frac{\nu}{D_B},\qquad N_b=\frac{(\rho c)_pD_B(\phi_w-\phi_\infty)}{\nu(\rho c)_f},$$
$$\mathrm{Pr}=\frac{\nu}{\alpha},\qquad N_t=\frac{(\rho c)_pD_T(T_w-T_\infty)}{\nu T_\infty(\rho c)_f}.$$

It is important to note that problem in Eq. (2.1b) is the same as considered by Attia [13]. Furthermore setting $N_b=0=N_t$ in Eq. (2.4b) provides the classical energy equation and by putting $N_b=0$ in Eq. (2.4c) one obtains the classical Fick's law.

The skin friction coefficient C_f, the local Nusselt number Nu and the local Sherwood number Sh are defined by

$$C_f=\mu\Big(\frac{\partial u}{\partial z}\Big)\Big/\rho_f(U_w)^2|_{z=0}, \tag{2.5a}$$

$$Nu=\frac{rq_w}{k(T-T_\infty)}, \tag{2.5b}$$

$$Sh=\frac{rj_w}{D(C-C_\infty)}, \tag{2.5c}$$

where q_w and j_w are the heat and mass fluxes respectively, which have the following values

$$q_w=-k\Big(\frac{\partial T}{\partial z}\Big)_{z=0,}\quad j_w=-D_B\Big(\frac{\partial C}{\partial z}\Big), \tag{2.6}$$

where k is the thermal conductivity of the fluid.

Together with Eqs. (2.5a)-(2.5c), Eqs. (2.6) become

$$=Re_r^{-1/2}f''(0),\quad Nu/Re_r^{1/2}=-\theta'(0),\quad Sh/Re_r^{1/2}=-\phi'(0), \tag{2.7}$$

where $Re_r(=cr^2/\nu)$ is the local Reynolds number.

3 Methodology

The nonlinear differential system given in Eqs. (2.4a)-(2.4c) is solved by homotopy analysis method (HAM) which is a powerful tool to solve nonlinear boundary value problems and has been used by many researchers [22–26]. The initial guesses f_0, θ_0 and ϕ_0 are selected in the following forms

$$f_0(\eta)=A\eta+(1-A)(1-\exp(-\eta)),\quad \theta_0(\eta)=\exp(-\eta),\quad \phi_0(\eta)=\exp(-\eta), \tag{3.1}$$

and linear operators are given by

$$\pounds_f=\frac{d^3f}{d\eta^3}-\frac{df}{d\eta},\quad \pounds_\theta=\frac{d^2\theta}{d\eta^2}-\theta,\quad \pounds_\phi=\frac{d^2\phi}{d\eta^2}-\phi. \tag{3.2}$$

Above linear operators satisfy the following properties

$$\pounds_f[C_1+C_2\eta+C_3\exp(-\eta)]=0, \tag{3.3a}$$
$$\pounds_\theta[C_4+C_5\exp(-\eta)]=0, \tag{3.3b}$$
$$\pounds_\phi[C_6+C_7\exp(-\eta)]=0. \tag{3.3c}$$

3.1 Zeroth-order deformation problems

The corresponding problems at this order are

$$\left.\begin{array}{l}(1-q)\pounds_f[\hat{f}(\eta;q)-f_0(\eta)]=q\hbar_f\mathcal{N}_f[,\hat{f}(\eta;q)],\\ \hat{f}(0;q)=0,\quad \dfrac{\partial\hat{f}(\eta;q)}{\partial\eta}\Big|_{\eta=0}=1,\quad \dfrac{\partial\hat{f}(\eta;q)}{\partial\eta}\Big|_{\eta\to\infty}=A,\end{array}\right\} \tag{3.4a}$$

$$\left.\begin{array}{l}(1-q)\pounds_\theta[\hat{\theta}(\eta;q)-\theta_0(\eta)]=q\hbar_\theta\mathcal{N}_\theta[\hat{\phi}(\eta;q),\hat{\theta}(\eta;q),\hat{f}(\eta;q),],\\ \hat{\theta}(\eta;q)|_{\eta=0}=1,\quad \hat{\theta}(\eta;q)|_{\eta\to\infty}=0,\end{array}\right\} \tag{3.4b}$$

$$\left.\begin{array}{l}(1-q)\pounds_\phi[\hat{\phi}(\eta;q)-\phi_0(\eta)]=q\hbar_\phi\mathcal{N}_\phi[\hat{\theta}(\eta;q),\hat{\phi}(\eta;q),\hat{f}(\eta;q),],\\ \hat{\phi}(\eta;q)|_{\eta=0}=1,\quad \hat{\phi}(\eta;q)|_{\eta\to\infty}=0,\end{array}\right\} \tag{3.4c}$$

in which $q\in[0,1]$ is the embedding parameter and $\hbar_f$, $\hbar_\theta$ and $\hbar_\phi$ are non-zero auxiliary parameters. Nonlinear operators $\mathcal{N}_f$, $\mathcal{N}_\theta$ and $\mathcal{N}_\phi$ are

$$\mathcal{N}_f[f(\eta,p)]=\frac{\partial^3 f(\eta,p)}{\partial\eta^3}-\Big(\frac{\partial f(\eta,p)}{\partial\eta}\Big)^2+2\bar{f}(\eta,p)\frac{\partial^2\hat{f}(\eta,p)}{\partial\eta^2}+A^2, \tag{3.5a}$$

$$\begin{aligned}\mathcal{N}_\theta[\hat{f}(\eta,p),\hat{\theta}(\eta,p),\hat{\phi}(\eta,p)]=&\hat{\theta}''(\eta,p)+2\mathrm{Pr}\hat{f}(\eta,p)\hat{\theta}'(\eta,p)+\mathrm{Pr}(N_b\hat{\theta}'(\eta,p)\hat{\phi}'(\eta,p)\\&+N_t(\hat{\theta}'(\eta,p))^2),\end{aligned} \tag{3.5b}$$

$$\mathcal{N}_\phi[\hat{f}(\eta,p),\hat{\theta}(\eta,p),\hat{\phi}(\eta,p)]=\hat{\phi}''(\eta,p)+2Le\hat{f}(\eta,p)\hat{\phi}'(\eta,p)+\frac{N_b}{N_t}\hat{\theta}''(\eta,p). \tag{3.5c}$$

3.2 Higher order deformation problems

The associated problems at this order are

$$\left.\begin{array}{l}\pounds_f[f_m(\eta)-\chi_m f_{m-1}(\eta)]=\hbar_f\mathcal{R}_m^f(f_{m-1}(\eta)),\\ f_m(0)=0,\quad f_m'(0)=0,\quad f_m'(\infty)=0,\end{array}\right\} \tag{3.6a}$$

$$\left.\begin{array}{l}\pounds_\theta[\theta_m(\eta)-\chi_{m\theta m-1}(\eta)]=\hbar_\theta\mathcal{R}_m^\theta(f_{m-1}(\eta),\theta_{m-1}(\eta),\phi_{m-1}(\eta)),\\ \theta_m(0)=0,\quad \theta_m(\infty)=0,\end{array}\right\} \tag{3.6b}$$

$$\left.\begin{array}{l}\pounds_\phi[\phi_m(\eta)-\chi_m\phi_{m-1}(\eta)]=\hbar_\phi\mathcal{R}_m^\phi(f_{m-1}(\eta),\theta_{m-1}(\eta),\phi_{m-1}(\eta)),\\ \phi_m'(0)=0,\quad \phi_m(\infty)=0,\end{array}\right\} \tag{3.6c}$$

$$\mathcal{R}_m^f(f_{m-1}(\eta),)=f_{m-1}'''(\eta)+\sum_{n=0}^{m-1}\left(\begin{array}{c}2f_n(\eta)f_{m-1-n}''(\eta)\\-f_n'(\eta)f_{m-1-n}'(\eta)\end{array}\right)+A^2(1-\chi_m), \tag{3.6d}$$

$$\begin{aligned}\mathcal{R}_m^\theta(f_{m-1}(\eta),\theta_{m-1}(\eta),\phi_{m-1}(\eta))=&\theta_{m-1}''(\eta)+\mathrm{Pr}\sum_{n=0}^{m-1}\left(\begin{array}{c}2f_n(\eta)\theta_{m-1-n}'(\eta)\\+N_b\hat{\theta}_n'(\eta)\phi_{m-1-n}'(\eta\end{array}\right)\\&+\mathrm{Pr}N_t\sum_{n=0}^{m-1}\theta_n'(\eta)\theta_{m-1-n}'(\eta),\end{aligned} \tag{3.6e}$$

$$\mathcal{R}_m^\phi(f_{m-1}(\eta),\theta_{m-1}(\eta),\phi_{m-1}(\eta))=\phi_{m-1}''(\eta)+2Le\sum_{n=0}^{m-1}f_n(\eta)\phi_{m-1-n}'(\eta)+\frac{N_b}{N_t}\theta_{m-1}'', \tag{3.6f}$$

where

$$\chi_m=\begin{cases}0, & m\le 1,\\ 1, & m>1.\end{cases}$$

The general solutions of problems consisting of Eqs. (2.4a)-(2.4c) are

$$f(\eta)=f^*(\eta)+C_1^m+C_2^m\eta+C_3^m\exp(-\eta), \tag{3.7a}$$

$$\theta(\eta)=\theta^*(\eta)+C_4^m+C_5^m\exp(-\eta), \tag{3.7b}$$

$$\phi(\eta)=\phi^*(\eta)+C_6^m+C_7^m\exp(-\eta), \tag{3.7c}$$

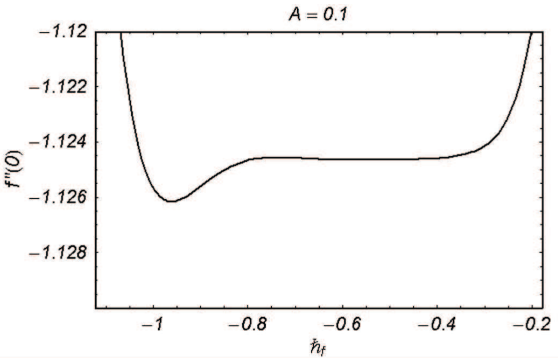

Figure 1: $\hbar_f$-curve for f''.

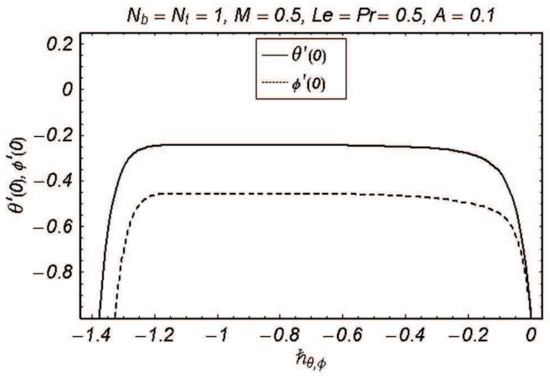

Figure 2: $\hbar_{\theta,\phi}$-curves for θ and ϕ.

where $f^*(\eta)$, $\theta^*(\eta)$ and $\phi^*(\eta)$ are the particular solutions of the problems given in the Eqs. (2.4a)-(2.4c).

The series solutions (3.7a)-(3.7c) contain auxiliary parameters $\hbar_f$, $\hbar_\theta$ and $\hbar_\phi$. The convergence of functions f, θ and ϕ strongly depend upon the auxiliary parameters $\hbar_f$, $\hbar_\theta$ and $\hbar_\phi$. In order to adjust and control the convergence of the developed solutions, we have plotted the $\hbar_{f,\theta,\phi}$-curves in Figs. 1 and 2. We note that range for admissible values of $\hbar_f$ and $\hbar_{\theta,\phi}$ are $-0.7 \leq \hbar_f \leq -0.4$ and $-1.2 \leq \hbar_{\theta,\phi} \leq -0.6$ respectively. Furthermore the series solutions converge up to $25th$ order of approximations (see Table 1).

4 Results and discussion

Nonlinear problems given in Eqs. (2.4a)-(2.4c) are solved by using homotopy analysis method (HAM). Velocity, temperature and mass fraction profiles against various values of dimensionless parameters are displayed (Figs. 3-9). Numerical values of the local skin friction coefficient, local Nusselt and Sherwood numbers are tabulated and analyzed for the effects of pertinent parameters (see Table 3). In order to validate the accuracy of our

Table 1: Convergence of the homotopy solutions for different order of approximation when $A=0.1$, $Le=\Pr=0.5$, $N_b=N_t=2$, $\hbar_f=-0.6$ and $\hbar_\theta=\hbar_\phi=-1$.

Order of approximation	$-f''(0)$	$-\theta'(0)$	$-\phi'(0)$
1	1.03500	0.008333	0.175000
5	1.12356	0.219163	0.401731
10	1.12463	0.241936	0.455136
15	1.12462	0.239161	0.454117
20	1.12461	0.238552	0.454419
25	1.12461	0.238407	0.454529
30	1.12461	0.238373	0.454561

results, we have given a comparative study between the present HAM solutions and existing numerical results [9]. An excellent agreement has been observed (see Table 2). Fig. 3 is plotted to examine the influence of stretching parameter A on radial velocity f'. $A>1$ corresponds to the case when free stream velocity is dominant whereas $A<1$ holds when stretching velocity is dominant. Interestingly an increase in A $(0\leq A<1)$ decreases velocity f' and the boundary layer thickness. However when the free stream

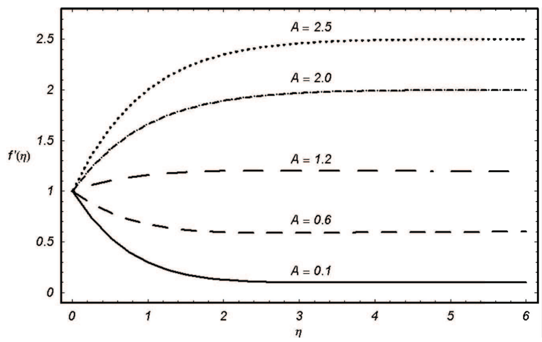

Figure 3: Influence of A on f'.

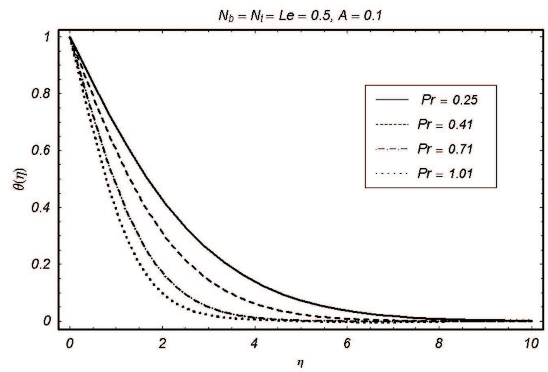

Figure 4: Influence of Pr on θ.

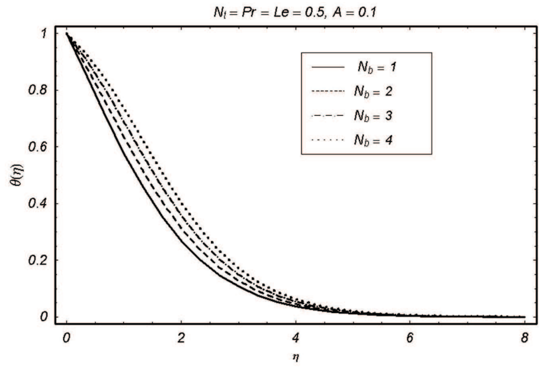

Figure 5: Influence of N_b on θ.

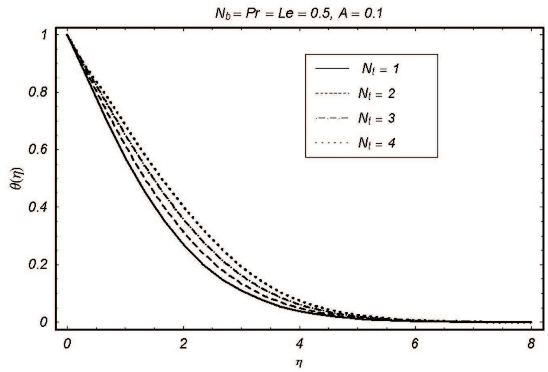

Figure 6: Influence of N_t on θ.

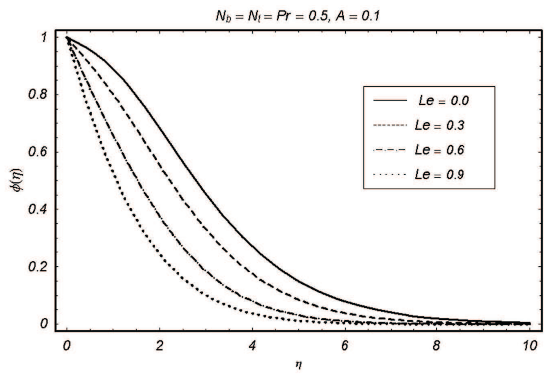

Figure 7: Influence of Le on ϕ.

velocity is greater than the stretching velocity, i.e., for $A > 1$, the velocity f' increases and the boundary layer thickness decreases. It means that the large values of A accompany with the higher free stream velocity giving rise to the velocity f'. Results of an increase in Pr on the temperature are observed in Fig. 4. In view of definition of Prandtl number (Pr $= v/\alpha$, the ratio of momentum diffusivity to thermal diffusivity), it con-

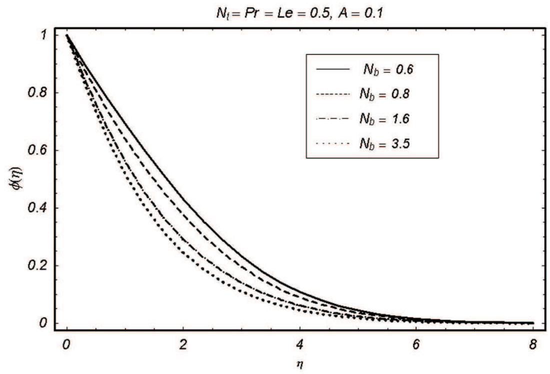

Figure 8: Influence of N_b on ϕ.

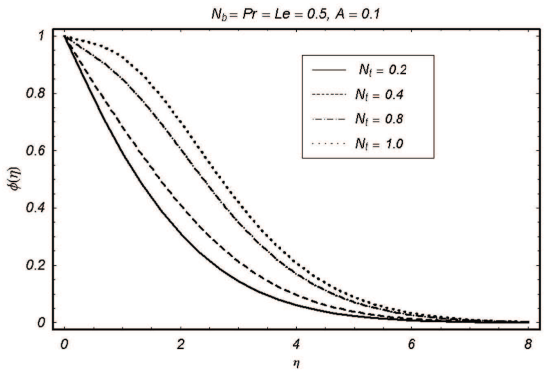

Figure 9: Influence of N_t on ϕ.

trols the relative thickness of the momentum and thermal boundary layers. Hence large Prandtl number means that velocity (momentum) diffuses quickly in comparison with heat and vice versa for small Pr. This shows that for liquid metals the thickness of the thermal boundary layer is much larger than the velocity boundary layer. It is note that for $N_b = N_t = 0$, Eq. (2.4b) reduces to energy equation for conventional fluid (base fluid). Fig. 5 elucidates that the effect of Brownian motion of nanoparticles on thermal conduction. This figure also indicates that Brownian motion of nanoparticles contributes to the thermal conduction enhancement and consequently temperature increases. It means that more heat conducts through nanofluids as compare to the conventional fluid. Thus use of nanoparticles in base fluid makes it possible to design coolants with industrial and biomedical applications in high-heat-flux cooling system. It is obvious from Fig. 5 that thermal boundary layer in nanofluid is higher than that of base fluid. It is observed form Fig. 6 that θ is an increasing function of N_t and so is the thermal boundary layer. The effect of Lewis number Le on mass fraction field ϕ is presented in Fig. 7. As Lewis number is defined as the ratio of thermal diffusivity to mass diffusivity and characterizes fluid flows where there is simultaneous transfer of heat and mass by convection. It is found from Fig. 7 that mass fraction field ϕ is a decreasing function of Le. It is noted from

Table 2: Comparison of the wall shear stress $f''(0)$ for different values of stretching parameter A.

	Ref [9]	Present case
A	$f''(0)$	
0.1	-1.1246	-1.12460
0.2	-1.0556	-1.05561
0.5	-0.7534	-0.75310
1.0	0.0000	0.00000
1.1	0.1821	0.18231
1.2	0.3735	0.36736
1.5	1.0009	1.02410

Table 3: Numerical values of the local skin friction coefficient $Re_r^{1/2}C_f$, the local Nusselt number $Re_r^{-1/2}Nu$ and the Sherwood number $Re_r^{-1/2}Sh$ for various values of physical parameters.

A	N_b	N_t	Pr	Le	$Re_r^{1/2}C_f$	$-Re_r^{-1/2}Nu$	$-Re_r^{-1/2}Sh$
0.0	2.0	2.0	0.5	0.5	1.17372	0.229072	0.374090
0.1	2.0	2.0	0.5	0.5	1.12460	0.238442	0.454496
0.2	2.0	2.0	0.5	0.5	1.05502	0.249055	0.509668
0.1	1	2.0	0.5	0.5	1.12460	0.318667	0.215940
0.1	2	2.0	0.5	0.5	1.12460	0.238442	0.454513
0.1	3	2.0	0.5	0.5	1.12460	0.175175	0.523783
0.1	2	0	0.5	0.5	1.12460	0.326795	0.561515
0.1	2	1	0.5	0.5	1.12460	0.278421	0.493110
0.1	2	2	0.5	0.5	1.12460	0.238442	0.454496
0.1	2	3	0.5	0.5	1.12460	0.205261	0.437014

Fig. 8 that an increase in N_t causes decrease in mass fraction field ϕ and the associated boundary layer whereas an increase N_b increases the mass fraction field ϕ (see Fig. 9). Table 3 is prepared to analyze the effects of some dimensionless parameters on the local skin friction coefficient, the local Nusselt number $(Re_r)^{-1/2}Nu_r$ and the local Sherwood number $(Re_r)^{-1/2}Sh_r$. This table depicts that local skin friction coefficient $(Re_r)^{1/2}C_f$ decreases when A is increased. The local Nusselt number $(Re_r)^{-1/2}Sh$ decreases whereas local Sherwood number $(Re_r)^{-1/2}Sh$ increases when N_b is increased. However N_t has similar effects on $(Re_r)^{-1/2}Nu$ and $(Re_r)^{-1/2}Sh$.

5 Final remarks

This research article discusses the axisymmetric stagnation-point flow of nanofluid over a stretching surface. Analytic solution of cuopled nonlinear boundary value problems is computed by homotopy analysis method (HAM). Derived solution in limiting case is compared with already exiting numerical solution. An excellent agreement between the present and already existing numerical results has been found. The whole analysis is summarized as:

1. Dimensionless velocity $f'(\eta)$ decreases when A increases through $(0,1)$. However opposite trend is noted for $A>1$.
2. Inclusion of nanoparticles in base fluid enhances its thermal conductivity. Therefore such fluids are used as coolants in industry and biomedical devices for high-heat-flux.
3. Dimensionless temperature θ is an increasing function of N_t and so is the thermal boundary layer.
4. An increase in N_t causes a decrease in mass fraction field ϕ and the associated boundary layer whereas an increase N_b increases the mass fraction field ϕ.
5. Dimensionless temperature θ is a decreasing function Prandtl number Pr and so is the thermal boundary layer thickness.

Acknowledgments

The first author is thankful to the Higher Education Commission (HEC) of Pakistan for the financial support under Startup Research Grant Program (SRGP). The authors are also grateful to the reviewer for his useful comments regarding earlier version of this manuscript.

References

[1] L. J. CRANE, *Flow past a stretching plate*, J. Appl. Math. Phys., 21 (1970), pp. 645–647.
[2] P. D. ARIEL, *Axisymmetric flow due to a stretching sheet with partial slip*, Comput. Math. Appl., 54 (2007), pp. 1169–1183.
[3] T. HAYAT, M. NAWAZ AND S. OBAIDAT, *Axisymmetric magnetohydrodynamic flow of a micropolar fluid between unsteady stretching surfaces*, Appl. Math. Mech. Engl. Ed., 32(2) (2011), pp. 361–374.
[4] T. HAYAT, M. NAWAZ, S. ASGHAR AND S. MESLOUB, *Thermal-diffusion and diffusion-thermo effects on axisymmetric flow of a second grade fluid*, Int. J. Heat Mass Trans., 54(13-14) (2011), pp. 3031–3041.
[5] T. HAYAT AND M. NAWAZ, *MHD flow of a micropolar fluid between the radially stretching sheets*, Zeitschrift für Naturforschung A, 66a (2011), pp. 53–60.
[6] T. C. CHIAM, *Stagnation-point flow towards a stretching plate*, J. Phys, Soc. Jpn., 63 (1994), pp. 2443–2444.
[7] T. R. MAHAPATRA, S. K. NANDY AND A. S. GUPTA, *Magnetohydrodynamic stagnation-point flow of a power-law fluid towards a stretching surface*, Int. J. Non-Linear. Mech., 44 (2009), pp. 124–129.
[8] F. LAPROPULU AND D. LI, *Stagnation-point flow of a second grade fluid with slip*, Int. J. Non-Linear Mech., 43 (2008), pp. 941–947.

[9] H. A. ATTIA, *Axisymmetric stagnation point flow towards a stretching surface in the presence of a uniform magnetic field with heat generation*, Tamkang J. Sci. Eng., 10(1) (2007), pp. 11–16.
[10] A. ISHAK, R. NAZAR, N. AMIN, D. FILIP AND I. POP, *Mixed convection in the stagnationpoint flow towards a stretching vertical permeable sheet*, Malaysian. J. Math. Sci., 2 (2007), pp. 217–226.
[11] T. HAYAT AND M. NAWAZ, *Unsteady stagnation point flow of viscous fluid caused by an impulsively rotating disk*, J. Taiwan Inst. Chem. Eng., 42(1) (2011), pp. 41–49.
[12] S. U. S. CHOI, Z. G. ZHANG, W. YU, F. E. LOCKWOOD AND E. A. GRULKE, *Anomalously thermal conductivity enhancement in nanotube suspensions*, Appl. Phys. Lett., 79 (2001), pp. 2252–2254.
[13] H. MASUDA, A. EBATA, K. TERAMEA AND N. HISHINUMA, *Altering the thermal conductivity and viscosity of liquid by dispersing ultra-fine particles*, Netsu Bussei, 4(4) (1993), pp. 227–233.
[14] S. DAS, *Temperature dependence of thermal conductivity enhancement for nanofluids*, J. Heat Trans., 125 (2003), pp. 567–574.
[15] B. C. PAK AND Y. CHO, *Hydrodynamic and heat transfer study of dispersed fluids with submicron metallic oxide particles*, Exp. Heat Trans., 11 (1998), pp. 151–170.
[16] J. A. EASTMAN, SU. S. CHOI, S. LI, W. YU, L. J. THOMPSON, *Anomalously increased effective thermal conductivity of ethylene glycol-based nanofluids containing copper nanoparticles*, Appl. Phys. Lett., 78(6) (2001), pp. 718–720.
[17] H. A. MINSTA, G. ROY, C. T. NGUYEN AND D. DOUCET, *New temperature dependent thermal conductivity data for water-based nanofluids*, Int. J. Thermal Sci., 48 (2009), pp. 363–371.
[18] P. RAZIA, M. A. AKHAVAN-BEHABADI AND M. SAEEDINIA, *Pressure drop and thermal characteristics of CuO–base oil nanofluid laminar flow in flattened tubes under constant heat flux*, Int. Commun. Heat Mass Trans., 38(7) (2011), pp. 964–971.
[19] P. RANA AND R. BHARGAVA, *Flow and heat transfer of a nanofluid over a nonlinearly stretching sheet*, Commun. Nonlinear Sci. Numer. Simul., 17 (2012), pp. 212–226.
[20] M. A. A. HAMAD AND M. FERDOWS, *Similarity solution of boundary layer stagnation-point flow towards a heated porous stretching sheet saturated with a nanofluid with heat absorption/generation and suction/blowing*, Commun. Nonlinear Sci. Numer. Simul., 17 (2012), pp. 132–140.
[21] M. ALINIA, D. D. GANJI AND M. GORJI-BANDPY, *Numerical study of mixed convection in an inclined two sided lid driven cavity filled with nanofluid using two-phase mixture*, Int. Commun. Heat Mass Trans., 38 (2011), pp. 1428–1435.
[22] S. J. LIAO, Beyond Perturbation: Introduction to Homotopy Analysis Method, Chapman and Hall, CRC Press, Boca Raton, 2003.
[23] M. M. RASHIDI, G. DOMAIRRY AND S. DINARVAND, *Approximate solutions for the Burger and regularized long wave equations by means of the homotopy analysis method*, Commun. Nonlinear Sci. Numer. Simul., 14(3) (2009), pp. 708–717.
[24] S. ABBASBANDY AND A. SHIRZADI, *A new application of the homotopy analysis method: Solving the Sturm–Liouville problems*, Commun. Nonlinear Sci. Num. Simul., 16 (2011), pp. 112–126.
[25] T. HAYAT, M. AWAIS AND S. OBAIDAT, *Three-dimensional flow of a Jeffery fluid over a linearly stretching sheet*, Commun. Nonlinear Sci. Numer. Simul., 17 (2012), pp. 699–707.
[26] I. HASHIM, O. ABDULAZIZ AND S. MOMANI, *Homotopy analysis method for fractional IVPs*, Commun. Non-linear Sci. Numer. Simul., 14 (2009), pp. 674–684.